Journal of Power Sources 195 (2010) 8052–8060

Contents lists available at ScienceDirect

Journal of Power Sources

journal homepage: www.elsevier.com/locate/jpowsour

Preparation, characterization and evaluation of proton-conducting hybrid membranes based on sulfonated hydrogenated styrene–butadiene and polysiloxanes for fuel cell applications

M. Monroy-Barreto[a], J.L. Acosta[b], C. del Río[b], M.C. Ojeda[b], M. Muñoz[c], J.C. Aguilar[a], E. Rodríguez de San Miguel[a], J. de Gyves[a,*]

[a] Departamento de Química Analítica, Facultad de Química, UNAM, Ciudad Universitaria, 04360 México, D.F., Mexico
[b] Instituto de Ciencia y Tecnología de Polímeros (CSIC), c/Juan de la Cierva 3, 28006 Madrid, Spain
[c] Departament de Química Analítica, Facultat de Ciències, U.A.B., Bellaterra 08193 Barcelona, Spain

ARTICLE INFO

Article history:
Received 21 May 2010
Received in revised form 30 June 2010
Accepted 30 June 2010
Available online 8 July 2010

Keywords:
Proton-conducting hybrid membranes
Sulfonation
Block copolymers
Sol–gel synthesis
PEMFC
Polarization curves

ABSTRACT

This paper describes the preparation of proton-conducting hybrid membranes (HMs) obtained by a solvent casting procedure using a solution containing sulfonated hydrogenated styrene–butadiene (HSBS-S) and an inorganic–organic mixture (polysiloxanes) previously prepared by a sol–gel route. HSBS-S copolymers with different sulfonation degrees were obtained and characterized by means of elemental analysis (EA), chemical titration and electrochemical impedance spectroscopy (EIS). HSBS-S with the best properties in terms of proton conductivity and solubility for the casting procedure was selected to prepare the HMs. The solvent casting procedure permitted the two phases to be homogeneously distributed while maintaining a relatively high proton conductivity in the membrane. HMs with different blend ratios were characterized using structural (Fourier transform infrared–attenuated total reflectance (FTIR–ATR), dynamic mechanical analysis (DMA), differential scanning calorimetry (DSC)), electrical (EIS), physicochemical (water uptake, ion-exchange capacity) and thermal (TGA–MS) methods. Finally, the optimized HSBS-S membrane and HMs were tested in hydrogen single fuel cells to obtain the polarization and power curves at different cell temperatures and gas pressures. Results indicate that HMs show a considerable improvement in performance compared to the optimized HSBS-S membrane denoting the benefit of incorporating the inorganic–organic network in the hydrogenated styrene–butadiene matrix. A Nafion membrane was used as reference material throughout this work.

1. Introduction

Block copolymers with multiple blocks of polystyrene connected by essentially elastomeric segments present highly processable characteristics (molding, casting, film formation) without the need for vulcanization chemicals. This behaviour is derived from their multiphase structure, i.e., polystyrene regions separated from each other by elastomeric segments [1]. Recently, sulfonated block copolymers have attracted much attention for the preparation of new proton-exchange membranes for fuel cell (PEMFC) applications [2], and several authors have reported such chemical modification with the aim of incorporating proton conductivity on block copolymers as a new feature with a view toward their use as electrolytes in these energy converting devices [3].

In addition, PEMFCs operating at high temperature are being pursued by researchers worldwide, because they have the advantage of enhanced tolerance to CO, accelerated reaction kinetics and significant improvement of the overall cell efficiency. Thus, membranes operating at high temperature and low relative humidity are needed. In this sense, one approach is the preparation of composite membranes formed by the incorporation of a basic inorganic structural material (filler) into an organic polymer matrix. In this type of material the components are usually held together by weak non-covalent interactions. The adsorbed water on the filler surface leads to an improved performance at higher temperatures [4].

It is well known that composite materials combining dissimilar organic and inorganic properties within a single material give rise to superior properties compared to their pure components. However, it is difficult to reach homogeneity at the molecular level for such materials. Weak chemical interactions between inorganic and organic units may lead to changes over long periods of time, such as aggregation, phase separation and bleeding. It is expected that these phenomena are diminished or even avoided with the

* Corresponding author.
E-mail address: degyves@servidor.unam.mx (J. de Gyves).

0378-7753/$ – see front matter © 2010 Elsevier B.V. All rights reserved.
doi:10.1016/j.jpowsour.2010.06.105

presence of stronger interactions, such as covalent bonds or by the simultaneous formation of interpenetrating networks between the inorganic and organic polymers that result in more homogeneous materials. One of the most promising procedures to meet this demand is the sol–gel process carried out under mild reaction conditions offering the possibility to form an inorganic network within a preformed organic polymer or even to carry out the organic polymerization either before, during or after the sol–gel route [5]. This paper describes the sulfonation of a commercial block copolymer (hydrogenated styrene–butadiene–styrene, HSBS) using acetyl sulfate. Products with different sulfonation degrees were obtained and characterized to evaluate the ion-exchange capacity and proton conductivity. The HSBS-S with the best properties in terms of proton conductivity and solubility for casting procedure was selected for hybrid membranes (HMs) preparation by a sol–gel process. This procedure allowed the two phases to be homogeneously distributed while maintaining high proton conductivity. The HMs were fully characterized by FTIR, DSC, DMA and electrochemical impedance spectroscopy (EIS). Finally, the HMs were tested in hydrogen single fuel cells and polarization and power curves at different temperatures and pressures were recorded. Results indicate that HMs show a considerably better performance as regards to the HSBS-S membrane.

2. Experimental

2.1. Reagents

Hydrogenated poly(butadiene–styrene) block polymer (HSBS) containing 30 wt% of styrene units was used, supplied by Repsol-YPF Química under the trade name of Calprene® H 6120. The sulfonating reagent consisted of acetic anhydride (98%) and sulfuric acid (95%), both from Panreac. The following solvents were used: 1,2-dichloroethane (99.5%, Scharlau), chloroform (99.95%, SDS), ethanol (99.9%, Merck) and isopropanol (99.5%, Scharlau). All solvents were used as received. HSBS was prepared by drying under vacuum for 5 h.

For hybrid membrane preparation, dichlorodimethylsilane ($Cl_2Si(CH_3)_2$, 97%, Sigma–Aldrich) was used as monomer; tetraethoxysilane ($Si(OC_2H_5)_4$ 98%, ABCR, TEOS) or phenyltrimethoxysilane (C_6H_5–$Si(OCH_3)_3$, 98%, Sigma–Aldrich PTMS) was used as a crosslinking agent. Ethyl ether $(C_2H_5)_2O$, 98%, Panrec), chloroform (99.95%, SDS), ethanol (99.9%, Merck) and dichloromethane (CH_2Cl_2, 99.5%, Fluka) were used as solvents. Na_2SO_4 (99.53%, J.T. Baker) was employed to remove excess water content. Nafion 117 solution (~5% in a mixture of lower aliphatic alcohols and water, Fluka) was used for the preparation of a reference membrane (Nafion-cast membrane).

2.2. Sulfonation reaction of HSBS

The HSBS-S copolymers were prepared according to a previously reported procedure [6]. A known weight (100 g) of the HSBS copolymer was dissolved in 750 mL of 1,2-dichloroethane and placed in a 4-necked reactor equipped with a mechanical stirrer, an addition funnel and nitrogen inlet and outlet. The mixture was then heated to 60 °C, and acetyl sulfate was added to the solution under vigorous stirring. Acetyl sulfate was previously prepared by mixing acetic anhydride (293 mL) and sulfuric acid (113 mL) in 1,2-dichloroethane (600 mL). Acetyl sulfate was maintained below 0 °C to prevent decomposition.

After acetyl sulfate incorporation was completed, samples were taken at several reaction times (65, 110 and 150 min) (Scheme 1). The addition of isopropyl alcohol inhibited further reaction and the sulfonated copolymer was immediately precipitated in boiling water. The precipitate was washed several times in an ultrafiltration cell with deionized water until neutral pH was obtained. Finally, the polymer was dried in a vacuum oven until constant weight was reached.

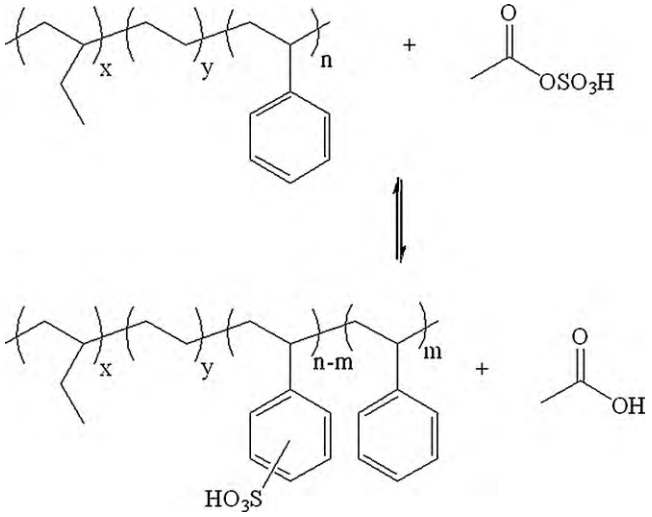

Scheme 1. Reaction scheme of HSBS sulfonation.

2.3. Preparation of silicon networks (silane phase, SP)

Silane phases were obtained by mixing dichlorodimethylsilane with diethyl ether in a 1:2 ratio and adding water to obtain a distinct aqueous phase, as previously described [7]. During hydrolysis, the reaction was kept cold to avoid a backlash that could lead to silica production. Both phases were separated; the remaining water in the organic phase was removed with sodium sulfate.

For crosslinking, TEOS and PTMS were used separately as crosslinking reagents. They were incorporated in the extracted phase containing the dichlorodimethylsilane derivative. The product obtained was a liquid mixture which was identified as silane phase (SP). If the hydrolysis reaction was allowed to continue, solution viscosity increased, ultimately leading to the production of a solid phase.

2.4. Preparation of membranes

HSBS-S membranes were prepared by solvent casting using chloroform–ethanol mixtures.

Hybrid membranes were prepared as follows: HSBS-S was dissolved in a chloroform:ethanol (90:10) mixture in order to have 2% (w/w) solutions. Then SP containing either TEOS (SPT) or PTMS (SPP) was added to the polymer solution. HMs with 70%, 80%, 90% and 95% (w/w) of the selected HSBS-S copolymer were prepared. In this work, hybrid membranes containing SPT and these HSBS-S proportions are identified as HSPT 70, HSPT 80, HSPT 90 and HSPT 95; and analog hybrid membranes containing SPP are named as HSPP 70, HSPP 80, HSPP 90 and HSPP 95.

For each hybrid membrane solution, the mixture was vigorously stirred for 1 h and then poured into a Teflon Petri dish to allow solvent evaporation at 48 °C.

2.5. Sulfonation and physicochemical analyses

Elemental analysis (EA) was performed in a LECO CHNS-932 analyzer in order to determine the concentration of elemental sulfur in the sulfonated copolymer.

For ion-exchange capacity determination (IEC, mequiv. H^+ g^{-1} polymer) the membranes were soaked in sodium chloride (3 M) for 24 h; afterwards, the solution was titrated against normalized NaOH solution (0.1 M) using phenolphthalein as indicator.

Water uptake was calculated by gravimetric analysis. Membranes were dried and their weight determined (W_{dry}). They were then immersed in distilled water at room temperature for 1 week to reach hydration equilibrium. Afterwards, the saturated wet membranes were carefully wiped and their weight measured (W_{wet}). Water absorption of the membranes was expressed as the percent ratio of weight increase using Eq. (1):

$$\text{water\_uptake}\,(\%) = \frac{W_{wet} - W_{dry}}{W_{dry}} \times 100 \quad (1)$$

2.6. Structural characterization

FTIR–ATR spectra were collected in the 4000–650 cm^{-1} range using a Perkin Elmer Spectrum GX spectrometer. Spectra were recorded using 25 scans at 4 cm^{-1} resolution.

Thermal behavior was analyzed on a Mettler TC15 differential scanning calorimeter (DSC). First, samples were cooled to −100 °C and maintained at this temperature for 5 min. Thermograms were recorded from −100 to 300 °C at a heating rate of 30 °C min^{-1} under nitrogen atmosphere. Two scans were performed for each sample.

This technique was also used to detect the state of the water absorbed in the hybrid membranes. A wet membrane (about 10 mg) was hermetically sealed in a sample pan and immediately cooled inside the DSC to −50 °C; it was held at this temperature for 3 min followed by the temperature raised to 50 °C at a heating rate of 5 °C min^{-1}.

Thermal stability was studied in a high-resolution thermobalance (TA instrument, TGA-Q500) coupled with a mass spectrometer (Omnistar/Pfeiffer Vacuum) for on-line evolved gas monitoring. Samples (about 10 mg) were heated at 10 °C min^{-1} to 820 °C under a helium atmosphere.

Dynamic mechanical analysis (DMA) was carried out on a Mettler Toledo DMA 861 analyzer operating in the tension mode. Spectra were recorded at a frequency of 10, 20 and 25 Hz within a temperature range from −100 to 300 °C, and at a heating rate of 3 °C min^{-1}.

Scanning electron microscopy (SEM) images of the hybrid membrane were acquired using a Philips XL30 electron microscope. Chemical compositions of the membranes were analyzed by using energy-dispersive X-ray with a sapphire detector having a super ultrathin window (SUTW) installed in the XL-30 FEG SEM apparatus. The membrane samples were fractured under cryogenic conditions.

2.7. Electrical characterization

Proton conductivity was determined at room temperature after 2 h of hydration by means of electrochemical impedance spectroscopy (EIS) in a Hewlett-Packard 4192-LF impedance analyzer. A frequency range from 10^{-2} to 10^4 kHz was used at an amplitude of 0.1 V. Proton conductivity of the membranes was calculated with Eq. (2) using the measured membrane resistance:

$$\sigma = \frac{L}{RA} \quad (2)$$

where σ is the material electrical conductivity (S cm^{-1}), L is the membrane thickness (cm), R is the measured membrane resistance (Ω) and A is the geometric membrane area (cm^2).

2.8. Performance tests

Performance tests of the membranes were carried out using a single-cell test station for PEMFC. The gases (H_2 and O_2) were humidified prior to entering the cell, being forced to pass through temperature-controlled water baths heated at 60 °C; the tests were run at two different operating pressures (1 and 2 bar) and three cell temperatures (60, 70 and 80 °C). The experimental single-cell from ElectroChem with an active area of 5 cm^2 consists of two graphite separator plates with serpentine flow pattern, silicon gaskets with high-precision thickness and heaters. Regarding the electrodes, the gas diffusion layer was Toray carbon paper (40 wt% wet proofing) and the catalyst layer had a platinum load of no less than 0.7 mg cm^{-2} (typically 0.78 ± 0.07 mg Pt cm^{-2}) using for its preparation 40% platinum on Vulcan XC-72 (E-TEK), 30% Nafion (5% solution, Fluka) and 2:1 isopropanol water as dispersion media. After sonicating, the catalyst ink was sprayed onto the gas diffusion layer using an automatic spraying system.

2.9. Hydrogen crossover

The H_2 crossover was measured at 60, 70 and 80 °C by potential-step voltammetry (potentiostat Autolab PGStat 30) supplying humidified H_2 and N_2 gases to the cell (50 mL min^{-1}). The anode served as the reference standard hydrogen electrode and the cathode as the working electrode. The potential was stepped from 0.2 to 0.5 V in 0.1 V increments of 180 s duration each. The steady-state current density (I_L) corresponds to the H_2 crossover through the membrane.

3. Results and discussion

3.1. Characterization of the HSBS-S membranes

Based on the results listed in Table 1, it is clear that the sulfonation degree (SD) strongly depends on the reaction time [8] and that it rises gradually as reaction time increases. From further experiments it was observed that relatively high sulfonation degrees lead to a proportional increase in interaction with water, lack of membrane strength and poor solubility in polar solvents [9,10]. Consequently, some properties, such as conductivity and ion-exchange capacity (IEC), could not be measured for the copolymer obtained from reaction 1 due to unsuccessful efforts to prepare the membranes. However, short reaction times (reaction 2) produced copolymers with low proton conductivities. For these reasons, the sulfonated copolymer obtained from reaction 3, which shows good conductivity, appropriate solubility for use in the casting procedure and ease of handling, was selected for characterization and subsequent preparation of hybrid membranes.

Table 1
Properties of HSBS-S copolymers.

Reaction	Reaction Time (min)	% *S*	Theoretical value (mequiv. g^{-1})	SD (mol%) (EA)	IEC (mequiv. g^{-1})	Conductivity (S cm^{-1})
1	150	5.41 ± 0.22	1.69	59.1	ND[a]	ND
2	65	3.05 ± 0.01	0.95	33.4	0.76 ± 0.03	0.005 ± 1e−4
3	110	3.44 ± 0.03	1.08	37.6	1.02 ± 0.01	0.010 ± 7e−5

[a] Not determined.

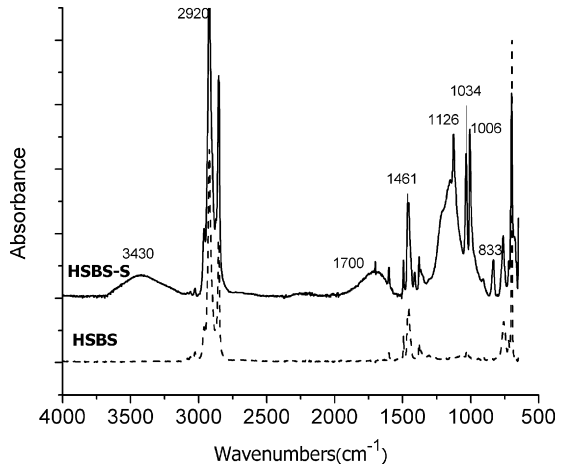

Fig. 1. FTIR–ATR spectra of HSBS and HSBS-S.

The selected sulfonated copolymer (HSBS-S) presents an excellent match between elemental analysis (EA) (3.44% sulfur content) corresponding to 1.08 mequiv. SO_3^- g^{-1} sample and IEC (1.02 mequiv. SO_3^- g^{-1}). This implies that the total sulfur determined by elemental analysis corresponds to the sulfonic groups present in the copolymer and are apparently available for ion-exchange. The proton conductivity value found for this HSBS-S membrane (0.01 S cm^{-1}) was measured by EIS at room temperature after 2 h of hydration. The water uptake of HSBS-S membrane was 81%.

FTIR was used to confirm the successful sulfonation reaction of HSBS. In Fig. 1 the FTIR spectra of HSBS and HSBS-S are presented. It is clear that both spectra show characteristic peaks of aliphatic compounds (ν_{C-H} 2920 cm^{-1} and ν_{C-H} 2852 cm^{-1}) and aromatic compounds (δ_{C-H} 3025 cm^{-1}, ν_{C-H} 2950 cm^{-1}, ν_{C-C} 1600 cm^{-1} and δ_{C-H} 699 cm^{-1}). However, new peaks can be observed for HSBS-S that are absent in the spectrum of the HSBS. In particular, six different peaks were identified and associated with the sulfonic acid groups (SO_3H) in the sulfonated copolymer. A broad absorption peak at around 3400 cm^{-1} indicates that a significant number of –OH groups are present due to the hydrogen bonding between SO_3H groups and absorbed water molecules [11]. The broad band at about 1700 cm^{-1} can be explained as a hydrogen bonding effect among SO_3H groups [12]. Peaks at 1150 and 1034 cm^{-1} are, respectively, assigned to the asymmetric and symmetric stretching vibrations (O=S=O) of sulfonic groups [13]. Finally, the peaks at 1006 and 1126 cm^{-1} can be assigned to in-plane bending vibrations of a *para*-substituted aromatic ring with a SO_3H group and to the sulfonate anion attached to the aromatic ring, respectively [14].

Block copolymers of polybutadiene and polystyrene exhibit two distinct glass transition temperatures (T_gs) that are close to the T_gs of the individual homopolymers. In the same way, HSBS show one T_g at low temperature corresponding to the rubbery "soft" segments of hydrogenated polybutadiene homopolymer (T_g^{HPB}) and another T_g at high temperature, corresponding to the rigid "hard" segments of polystyrene (T_g^{PS}) [15,16]. Fig. 2 shows the DSC thermograms recorded for HSBS and HSBS-S during the first and second heating stages, respectively. T_g^{HPB} appears at about −52 °C for both copolymers which confirms that sulfonation does not modify the polybutadiene segments [3], as was expected, since the electrophilic substitution reaction only takes place in the benzene rings of polystyrene phase [17]. In Fig. 2a the strong endothermic transition centered at 142 °C, that is not present in HSBS, is related to the breakdown of the ionic aggregations or cluster phase and therefore, can be assigned to the presence of sulfonic groups in the copolymer chains [18]. Moreover, this transition is not observed in the second heating scan (Fig. 2b).

Previous research [19] has reported that the introduction of sulfonic groups increases not only the molecular bulkiness but also the interactions between macromolecular chains by the hydrogen bonding effect of SO_3H groups (ionomer effect); thus the SO_3H groups on adjacent chains may easily interact by forming hydrogen bonds [20]. It is likely that these intermolecular forces hinder the internal motions compared to the HSBS copolymer. Thus, T_g^{PS} increases considerably (+50 °C) after sulfonation, with $T_g^{PS} = 97$ °C for HSBS and 148 °C for HSBS-S (Fig. 2b). This important increase in glass transition temperature is directly associated with sulfonic content.

Thermal stability and degradation of the HSBS and HSBS-S copolymers were studied by thermogravimetric–mass spectroscopy analysis (TGA–MS). Figs. 3 and 4 show TGA–MS spectra for HSBS and HSBS-S, respectively, exhibiting different profiles. In the case of HSBS, the thermal degradation started at 319 °C. Jang and Wilkie [21] report that the degradation pathway of polystyrene proceeds by chain cleavage followed by depolymerization and formation of the main evolved products: styrene monomer, dimer, and trimer. The evolved gases during the thermal degradation of HSBS were identified through MS analysis of the fragments: m/z = 104 and 103 for styrene monomer and m/z = 78 and 77 for benzene. In the case of HSBS-S weight loss was determined by thermogravimetry and occurred in 3 consecutive steps. The first weight loss can be attributed to the release of atmospheric moisture that occurs as a result of the hygroscopic nature of the HSBS-S. The unusually high ionic charge of the sulfonic acid groups causes a strong ionic interaction with the absorbed water molecules, resulting in the release of water molecules over an extended temperature range between 100 and 200 °C. The second weight loss takes place between 200 and 350 °C and is due to the breakdown of the sulfonic groups

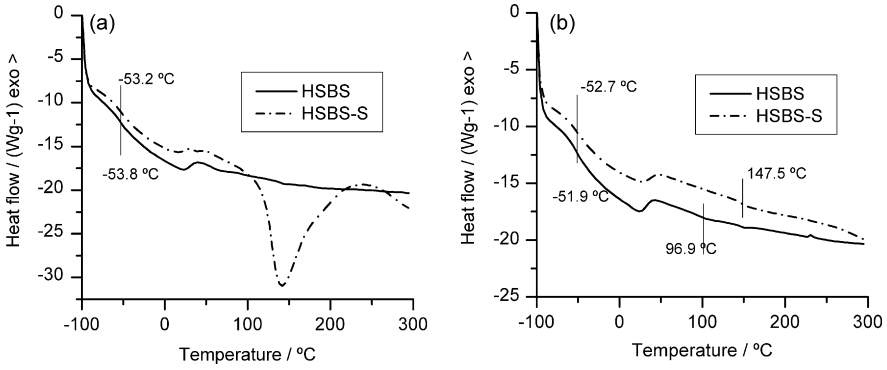

Fig. 2. DSC spectra for HSBS and HSBS-S: (a) first heating; (b) second heating.

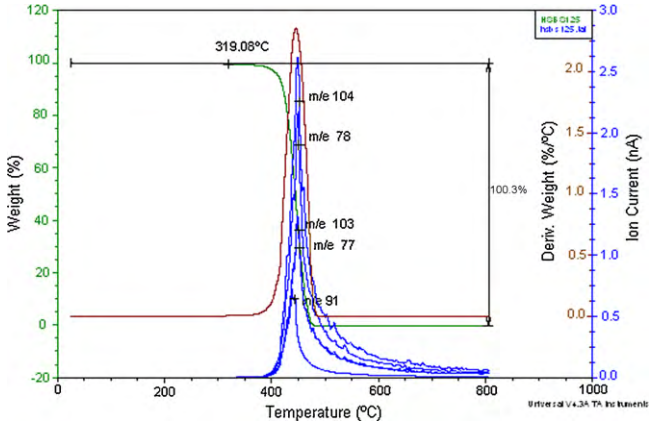

Fig. 3. Thermal degradation of HSBS. Mass trace of the evolution of main fragments.

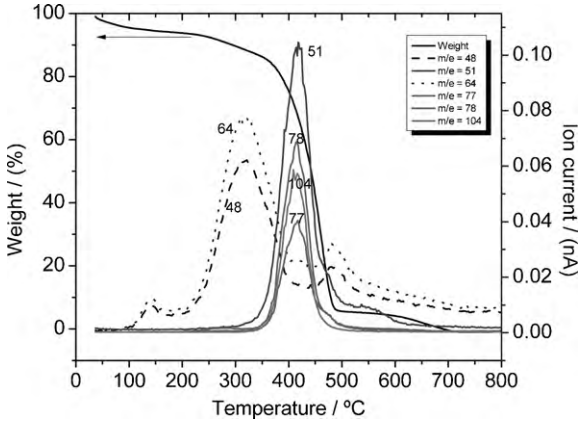

Fig. 4. Thermal degradation of HSBS-S. Mass trace of the evolution of main fragments.

attached to the styrene rings. The third and last weight loss occurs above 350 °C and corresponds to the degradation of the polymer chains [22]. This degradation temperature is higher than that of the HSBS and implies that the sulfonic acid attached to the skeleton of the copolymer increases its temperature of degradation. Thermal stability increase after sulfonation was observed in other studies with styrene copolymers and can also be attributed to the presence of residual double bonds in intermediate blocks resulting from incomplete hydrogenation of the butadiene-based precursor [23]. The most important gases involved in HSBS-S degradation were $m/z = 48$ (SO^+) and 64 (SO_2^+) derived from desulfonation and $m/z = 51$ ($C_4H_3^+$) from the main chain degradation; those resulting

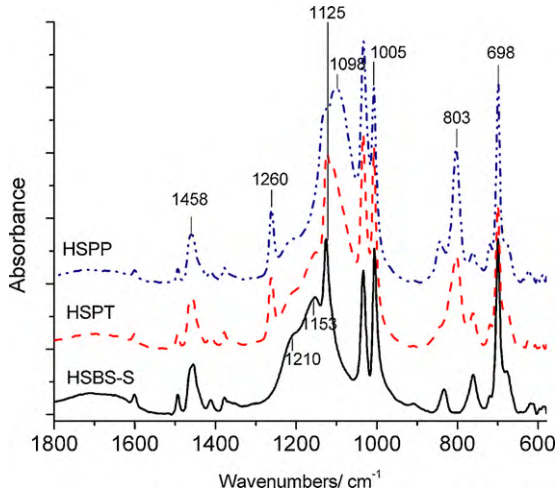

Fig. 5. FTIR–ATR spectra of HSBS-S membrane and hybrid membranes prepared with silane phases using TEOS and PTMS as crosslinking agents.

from benzene and styrene were $m/z = 77$ ($C_6H_5^+$), 78 ($C_6H_6^+$) and 104 ($C_8H_8^+$).

3.2. Hybrid membranes characterization

In the FTIR–ATR spectra of the hybrid membranes (Fig. 5) characteristic peaks of the sulfonated copolymer (Section 3.1) were observed. Furthermore, additional peaks derived from dichlorodimethylsilane [24] were located at 1260 and 803 cm^{-1}. They correspond to the symmetric bending vibration of methyl groups attached to the silicon atoms ($\delta(CH_3)$ $Si–CH_3$) and stretching vibrations of the silicon–carbon groups Si–C (ν(Si–C)), respectively. The spectra of the hybrid membranes also displayed a wide peak in the region of 1110–1050 cm^{-1} that does not appear in the sulfonated polymer. It corresponds to stretching vibrations of Si–O–Si and Si–O–C groups resulting from the sol–gel reaction between the dichlorodimethylsilane derivative and the crosslinking agent [25].

DSC experiments of hybrid membranes (Fig. 6) also disclose the presence of an endothermic transition centered around 150 °C. As previously stated, this transition is irreversible and has been assigned to the existence of sulfonic groups attached to the sulfonated copolymer chains. Fig. 6 also shows the DSC curves of hybrid membranes as a function of silane phase content. As the silane phase content was increased the endothermic peak area decreased indicating that the silane phases prevent association between sulfonic groups by changing the structure of ionic clusters [26].

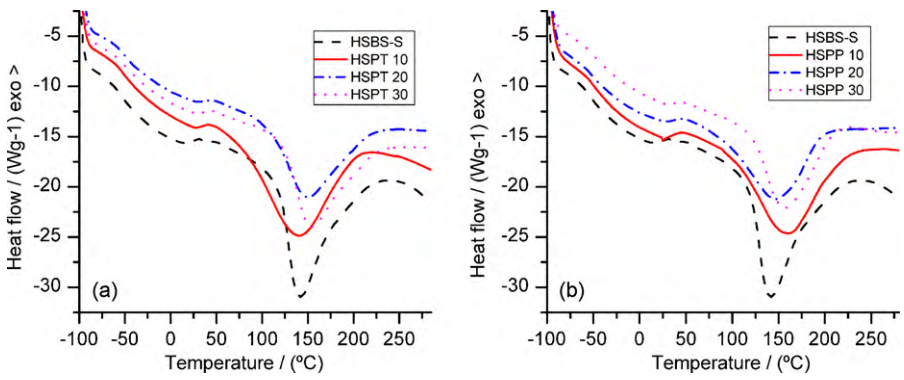

Fig. 6. Comparison of DSC curves obtained for the sulfonated copolymer (HSBS-S) and hybrid membranes prepared with silane phases using TEOS (a) and PTMS (b) as crosslinking agents.

Table 2
Water content in hybrid membranes.

Membrane	% total water (±3.5)	% freezable water (±0.9)	% bound water (±3.6)
HSBS-S	81	19	62
HSPT 90	51	36	16
HSPT 80	52	27	25
HSPT 70	46	18	28
HSPP 90	51	29	22
HSPP 80	54	28	26
HSPP 70	51	23	28

Table 3
DMA analysis for HSBS-S membranes.

Membrane	T_g^{HPB}	T_g^{PS}
HSBS-S	−40	171.5
HSPT 95	−37.5	172.2
HSPT 90	−36.6	170.4
HSPT 80	−40.2	172.6
HSPT 70	−33.3	174.0
HSPP 90	−37.3	177.8
HSPP 80	−39.9	172.7
HSPP 70	−37.9	199.3

It is well known that water molecules confined in membranes play an important role in determining transport properties such as proton conductivity [27], which in turn determine the membrane performance in a fuel cell [28]. Consequently, the hydrated membranes were studied by DSC in order to better understand the behavior of water molecules. Based on various thermodynamic properties of water absorbed in hydrophilic polymers, several authors have proposed that water is present in three forms: the first is non-freezing, bound water which is strongly attached to the polymer chain, and does not crystallize even when the swollen sample is cooled down to −100 °C [29]. In this case, it is often impossible to observe crystallization exotherms or melting endotherms for water fractions closely associated with the polymer matrix [30]. The second kind is freezing water which is weakly bound to the polymer chains and is able to be crystallized at a temperature lower than 0 °C. The third kind is free water which is not bound to the polymer and it is able to crystallize at 0 °C [26,31]. Quantification of each water state in the membrane using DSC is of great interest but is not an easy matter. One endothermic peak of water melting near 0 °C was observed in the DSC thermograms of all the membranes studied, corresponding to frozen water molecules. It is assumed that this type of water can be the same as free water. Thus, freezable water content is estimated on the basis of the assumption that the fusion enthalpy of this type of water is the same as that of free water (334 J g^{-1}). The results obtained for each of the membranes analyzed are shown in Table 2. Bound water can be calculated by the difference between the total water (or water uptake) and the freezing water content as is indicated in Eq. (3):

$$\text{Water}_{\text{bound}} = \text{Water}_{\text{total}} - \text{Water}_{\text{freezable}} \quad (3)$$

where $\text{Water}_{\text{bound}}$ represents the fraction of water strongly interacting with the membrane, $\text{Water}_{\text{total}}$ is the water uptake of the dry membrane and $\text{Water}_{\text{freezable}}$ is the water percentage non- or weakly interacting with the membrane (freezable water).

These results lead one to conclude that sulfonic groups provide high hydrophilicity to HSBS-S. Water uptake percentage increases up to 80%. However, the addition of a silane phase to the membranes decreases water absorption; this is attributed to the fact that since the silane phases are crosslinked they give greater rigidity to the membranes preventing further water diffusion with respect to HSBS-S membranes. With lower percentages of silane phase, freezable water amounts are higher; the opposite occurs with bound water which is attributed to OH groups from silane phase structure. As silane phase content goes up, the number of hydrophilic sites increases and allows stronger interactions of water molecules with the membrane.

As previously mentioned, HSBS-S exhibits two well-differentiated glass transition temperatures: (T_g^{HPB}) corresponding to hydrogenated butadiene phase and T_g^{PS} related to polystyrene-rich phase. DMA tan δ curves of hybrid membranes prepared with SPT and SPP are presented in Fig. 7.

Observing tan δ curves for hybrid membranes prepared with SPT as crosslinking agent, the peaks corresponding to flexible elastomeric hydrogenated polybutadiene phase shifted slightly towards higher temperatures when the amount of SPT was varied from 0 to 5, 10, 20 and 30% (w/w) against the HSBS-S matrix. However, the relaxations associated to T_g^{PS} do not change significantly. As regards the hybrid membranes prepared with SPP the opposite effect is observed. In this case, the peaks corresponding to the polybutadiene phase remained almost constant while the relaxations corresponding to polystyrene phase were shifted to higher temperatures and were also broadened. This is directly attributed to membranes crosslinking since by increasing the silane phase content the flexibility restriction of the chains is enhanced. Therefore, it is possible to state that SPT interacts more with hydrogenated polybutadiene regions and SPP with the polystyrene regions. Table 3 summarizes the resulting values from the respective relaxations regarding the butadiene and polystyrene phases at 10 Hz.

The silane phase distribution was studied using a scanning electron microscope (SEM) coupled with an energy-dispersive X-ray (EDX) probe that allowed the determination of the local chemical composition of the samples.

In order to obtain an overall image of the distribution of the silane phase in the hybrid membranes, the surface was analyzed at different points and a cross-section was analyzed at different sur-

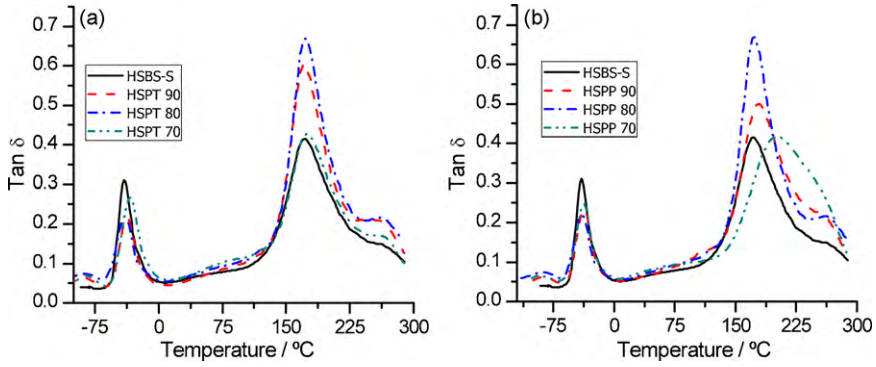

Fig. 7. tan δ curves at 10 Hz of HSBS-S and hybrid membranes with the indicated SPT/HSBS-S (a) and SPP/HSBS-S (b) compositions.

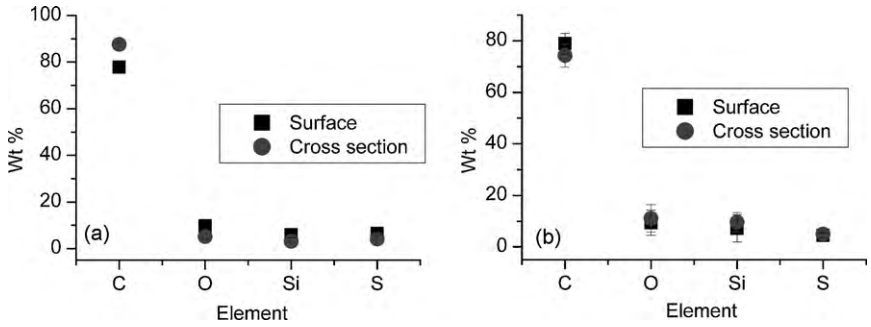

Fig. 8. EDX analysis of the hybrid membranes prepared with SPT (a) and SPP (b).

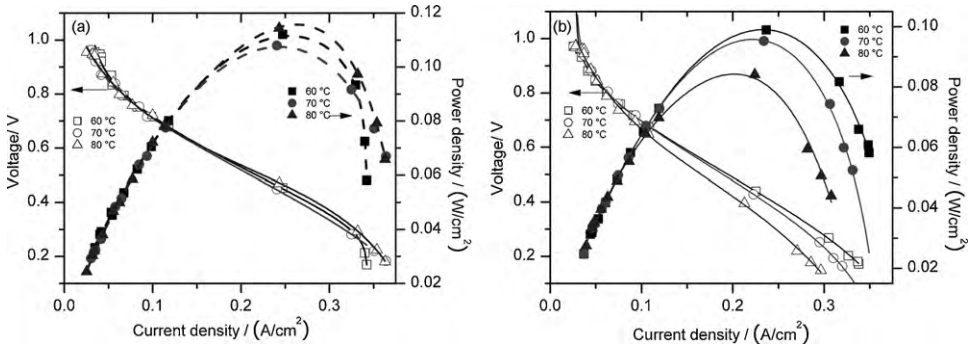

Fig. 9. Polarization curves of membranes prepared with (a) SPT 10% and (b) SPP 10%.

face levels (Fig. 8). Elemental analysis was further performed on the surface layer in order to identify the chemical components by EDX analysis. The elements C, O, Si and S were detected, showing a steady distribution, indicating that the silane phases are homogeneously located within the membrane.

3.3. Performance test

It is a common practice to test fuel cell performance by working with H_2/O_2 at different temperatures and pressures, as well as by determining polarization curves and power density. In Fig. 9, the single-cell behavior is shown for membranes HSPT90 and HSPP90 at 1 bar and different temperatures. Behavior is synthesized in the graph with its current *vs* potential characteristics. The liberated power (P) of a fuel cell is given by the product of current and voltage:

$$P = iV \quad (4)$$

All I–V curves show the output voltage of the fuel cell for a given current. For the synthesized membranes, a voltage reduction at low current densities is observed. This is probably due to losses by activation because of electrochemical reactions, since the current generated by the fuel cell is directly related to electrochemical reactions velocities.

With current densities slightly higher than 0.1 A cm^{-2}, ohmic losses caused by ionic and electronic conduction become important and losses by activation are not meaningful. In this zone, voltage falls in a soft way and it is in this zone where the membrane inner resistance acts as an important factor.

At high current density (0.28 A cm^{-2}), losses by concentration due to mass transport are observed in some cases.

Table 4 compares experimental maximum power density values obtained for Nafion-cast, HSBS-S and the prepared hybrid membranes.

As shown in Table 4, it is clear that all maximum power densities measured for the membranes synthesized with HSBS-S are lower than those Nafion-cast or Nafion 117 commercially available membranes [32] in spite of thickness difference. Also, it is worth noting that the addition of a silane phase to the membranes yields to a better performance by increasing the power density as compared to HSBS-S alone. The highest power density values were obtained for

Table 4
Maximum power densities values for Nafion-cast, HSBS-S and prepared hybrid membranes.

Membrane	Thickness (μm)	Power density$_{max}$ (mW cm^{-2}) P = 1 bar			Power density$_{max}$ (mW cm^{-2}) P = 2 bar		
		60 °C	70 °C	80 °C	60 °C	70 °C	80 °C
Nafion-cast	80	120	118	106	130	129	124
HSBS-S	41	75	75	66	74	67	59
HSPT 95	55	92	86	72	89	80	82
HSPT90	44	112	108	115	118	107	103
HSPT80	80	86	90	80	77	71	58
HSPT70	40	60	53	ND[a]	60	59	52
HSPP95	40	95	84	63	102	94	80
HSPP90	45	99	95	84	83	82	71
HSPP80	51	78	40	ND	83	83	79
HSPP70	65	50	ND	ND	ND	ND	ND

[a] Not determined.

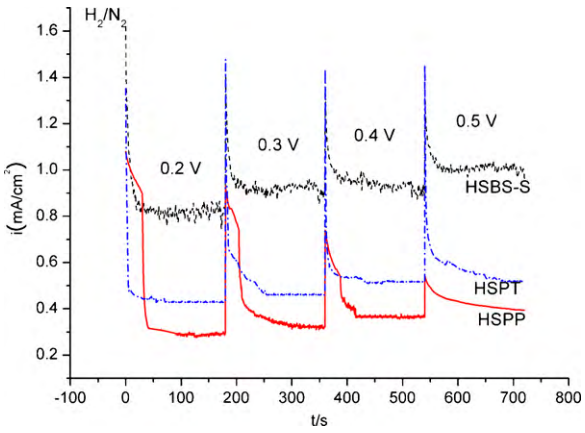

Fig. 10. Potential-step voltammograms of HSBS-S membrane and hybrid membranes, at 70 °C.

those membranes prepared with a 10% of SPT, thus it is observed that values remain more or less stable, except for the experiment performed at 2 bar and 80 °C, where the power density decreases slightly.

3.4. Hydrogen crossover

Finally, the hydrogen crossover in a fuel cell is produced by the unwanted diffusion of hydrogen through the membrane from the anode to the cathode. This phenomenon causes a lower open-circuit voltage in PEMFCs [33]. The hydrogen crossover using the HSBS-S membranes prepared in this work was estimated by means of potential-step voltammetry supplying humidified H_2 and N_2 gases. The observed limiting current densities (i_L) are due to hydrogen oxidation in the working electrode (the cathode of the fuel cell) the anode acting as the reference standard hydrogen electrode (SHE) [34]. The linear fit when plotting limiting current densities as a function of working electrode potential contributes the following information:

The linear interpolation of the data to the *y*-axis represents the limiting current density for hydrogen oxidation at the cathode, i_{H_2Ox}, and the inverse slope indicates the electronic resistance of the system due to the electrons crossing the membrane.

When the limiting current density for hydrogen oxidation at the cathode i_{H_2Ox} is lower than 2 mA cm^{-2}, the loss of cell efficiency caused by H_2 crossover can be considered negligible and values of electronic resistance higher than 300 Ω cm^2 indicate that the possible electronic leakage has no effect on the cell performance [35]. It is interesting to note that the hydrogen crossover is reduced with the addition of the silane phases, as shown in Fig. 10 and Table 5. This effect can be attributed to the fact that the use of the silane phases gives rise to a more rigid membrane structure, inhibiting hydrogen diffusion through the hybrid membrane in contrast to the HSBS-S membrane alone. Furthermore, hydrogen crossover is higher in hybrid membranes prepared with SPP than those prepared with SPT, due to the presence of the more voluminous phenyl group in the former.

Table 5
Chronoamperometric values obtained for HSBS-S and hybrid membranes.

Membrane	i_{H_2Ox} (mA cm^{-2})			Electronic resistance (Ω cm^{-2})		
	60 °C	70 °C	80 °C	60 °C	70 °C	80 °C
HSBS-S	0.567	0.713	ND[a]	3109	1701	ND
HSPT 90	0.074	0.217	ND	1424	2747	ND
HSPP 90	0.230	0.366	0.539	2688	3049	2092

[a] Not determined.

4. Conclusions

Sulfonated hydrogenated styrene–butadiene copolymers (HSBS-S) with different sulfonation degrees were synthesized. It was observed that sulfonation degree increases with reaction time; however, longer reaction times give raise to a product that does not result in a useful membrane. The HSBS-S copolymer obtained at moderate reaction time (112 min) exhibited an acceptable sulfonation degree (3.44 ± 0.03%) with the highest conductivity and presented excellent solubility in the casting medium to form hybrid membranes (HMs) with inorganic–organic phases of TEOS or PTMS. Results obtained from FTIR–ATR, elemental analysis, IEC, TAN, conductivity and DSC studies indicated that the sulfonic groups in the polymer chain are covalently attached and fully available for proton exchange, as deduced from comparing its theoretical ion-exchange capacity (1.08 mequiv. SO_3^- g^{-1}) with that obtained by titration (1.02 mequiv. SO_3^- g^{-1}). These sulfonic groups generate hydrophilic sites that favor maintaining a proton conductivity of 0.010 S cm^{-1}. It was possible to form HMs with HSBS-S and TEOS (HSPT) or PTMS (HSPS) at different blend ratios (70–95%, w/w of HSBS-S). Their chemical characterizations indicated that the silane phase (SP) is homogenously distributed along the matrix, that TEOS interacts more strongly with the polybutadiene region of HSBS-S while PTMS interacts with the polystyrene regions, and that sulfonic groups provide high hydrophilicity to HSBS-S allowing a water uptake of 81%. The HMs were thermally stable up to 170 °C and according to DMA results mechanically stable. In relation to HMs performance in the single-cell set-up, an increase in the power density for HSPT and HSPP in comparison with HSBS-S membranes was observed. The HSPT membranes perform better than HSPP but not as well as Nafion. Interestingly, hydrogen crossover was reduced by incorporation of the silane phase, being higher in HSPP than HSPT.

Acknowledgements

This work was supported by DGAPA-UNAM (project IN102508) and CONACYT (project 81313). M. Monroy gratefully thanks CONACYT for doctoral scholarships.

Spanish project (MEC ENE2007-62791/ALT) is gratefully acknowledged for financial support.

References

[1] M. De Sarkar, P.P. De, A.K. Bhowmick, J. Appl. Polym. Sci. 66 (1997) 1151–1162.
[2] W.H. Choi, W.H. Jo, J. Power Sources 188 (2009) 127–131.
[3] A. Navarro, C. Del Río, J.L. Acosta, J. Membr. Sci. 300 (2007) 79–87.
[4] M.L. Di Vona, D. Marani, A. D'Epifanio, E. Traversa, M. Trombetta, S. Licoccia, Polymer 46 (2005) 1754–1758.
[5] G. Kickrelbick, Hybrid Materials Synthesis, Characterization and Applications, Wiley–VCH Verlag, Germany, 2007.
[6] H.S. Makowski, S. Plains, R.D. Lundberg, J. Bock, Process for the sulfonation of an elastomeric polymer, US Patent 4,184,988 (1980).
[7] M. Monroy-Barreto, J.C. Aguilar, E. Rodriguez de San Miguel, A.L. Ocampo, M. Muñoz, J. de Gyves, J. Membr. Sci. 344 (2009) 92–100.
[8] P. Genova-Dimitrova, B. Baradie, D. Foscallo, C. Poinsignon, J.Y. Sanchez, J. Membr. Sci. 185 (2001) 59–71.
[9] D. Lu, H. Zou, R. Guan, H. Dai, L. Lu, Polym. Bull. 54 (2005) 21–28.
[10] R. Guan, H. Zou, D. Lu, C. Gong, Y. Liu, Eur. Polym. J. 41 (2005) 1554–1560.
[11] H.Y. Hwanga, H.C. Koh, J.W. Rhim, S.Y. Nam, Desalination 233 (2008) 173–182.
[12] B. Peres, L. Claudio de Santa Maria, M.E. Sena, Mater. Lett. 61 (2007) 2540–2543.
[13] S. Wang, Z. Zeng, S. Yang, L.-T. Weng, P.C.L. Wong, K. Ho, Macromolecules 33 (2000) 3232–3236.
[14] Y.A. Elabd, E. Napadensky, Polymer 45 (2004) 3037–3043.
[15] H. Daimon, H. Okitsu, J. Kumanotani, Polym. J. 4 (1975) 460–466.
[16] G.H. Michler, F.J. Baltá-Calleja, Mechanical Properties of Polymers Based on Nanostructure and Morphology, CRC Press, Boca Raton, 2005.
[17] F. Picchioni, I. Giorgi, E. Passaglia, G. Ruggeri, M. Aglietto, Polym. Int. 50 (2001) 714–721.
[18] A. Mokrini, J.L. Acosta, Polymer 42 (2001) 9–15.
[19] R. Guan, C. Gong, D. Lu, H. Zou, W. Lu, J. Appl. Polym. Sci. 98 (2005) 1244–1250.
[20] S.M.J. Zaidi, Arab. J. Sci. Eng. 28 (2003) 183–194.

[21] B.N. Jang, C.A. Wilkie, Polymer 46 (2005) 2933–2942.
[22] J.M. Sloan, D. Suleiman, E. Napadensky, D.M. Crawford, Thermo Stability of Highly Sulfonated Poly(styrene–isobutylene–styrene) Block Copolymers: Effects of Sulfonation and Counter-ion Substitution, Army Research Laboratory, 2008, ARL-TR-4357.
[23] R.F. Storey, B.J. Chisholm, Y. Lee, Polym. Eng. Sci. 37 (1997) 73–80.
[24] E.A. Abdel-Razik, Polym. Int. 40 (1996) 207–211.
[25] R.V. Gummaraju, R.B. Moore, K.A. Mauritz, J. Polym. Sci. Part B: Polym. Phys. 34 (1996) 2383–2392.
[26] S.H. de Almeida, Y. Kawano, J. Therm. Anal. Cal. 58 (1999) 569–577.
[27] D.S. Kim, K.H. Shin, H.B. Park, Y.S. Chung, S.Y. Nam, Y.M. Lee, J. Membr. Sci. 278 (2006) 428–436.
[28] Y.S. Kim, L. Dong, M.A. Hickner, T.E. Glass, V. Webb, J.E. McGrath, Macromolecules 36 (2003) 6281–6285.
[29] J. Zhang, H. Teng, X. Zhou, D. Shen, Polym. Bull. 48 (2002) 277–282.
[30] H. Hatakeyama, T. Hatakeyama, Thermochim. Acta 308 (1998) 3–22.
[31] Z.H. Ping, Q.T. Nguyen, S.M. Chen, J.Q. Zhou, Y.D. Ding, Polymer 42 (2001) 8461–8467.
[32] P.G. Escribano, C. del Río, J.L. Acosta, J. Power Sources 187 (2009) 98–102.
[33] C. Francia, S. Specchia, N. Penáis, P. Spinelli, II Iberian Symposium on Hydrogen, Fuel cells and Advanced Batteries, Vila Real, Portugal, September 13th–17th, 2009.
[34] Z. Xie, X. Zhao, M. Adachi, Z. Shi, T. Mashio, A. Ohma, K. Shinohara, S. Holdcroft, T. Navessin, Energy Environ. Sci. 1 (2008) 184–193.
[35] C. del Río, P.G. Escribano, E. Morales, M.A. Torre, M.C. Ojeda, F. Sánchez, J.L. Acosta, II Iberian Symposium on Hydrogen, Fuel Cells and Advanced Batteries, Vila Real, Portugal, September 13th–17th, Poster P15-SA, 2009.